

THE BEHAVIOUR OF THE JEFFCOTT ROTOR UNDER A VIBRATING BASE OF FLUID FILM BEARING

Hussien Mahmoud Al-Wedyan¹, Montasser Suliman Tahat¹ and Saad Assi Mutasher^{2*}

Received: Nov 28, 2007; Revised: Sept 16, 2008; Accepted: Sept 25, 2008

Abstract

The whirl motion of the Jeffcott rotor was investigated. The system was analyzed by setting up the kinetic, potential, and dissipation energy equations, and the excitation was assumed as a random vibration on the base of the fluid film bearing of the rotor. Lagrangian was used to derive the equations of motion in the Y and Z directions and the Simulink under Matlab software was used to simulate the current system. The simulation was carried out under a constant rotational speed and different masses for the shaft and the disk. In addition, the effect of changing the stiffness and the damping coefficients is also investigated. The responses of the two coordinates (Z and Y) were also observed as well as the whirl orbits of the shaft for different mass ratios. Furthermore, the stability of the system was investigated mathematically. The results show that the whirl motion is stable when the rotor speed is 8,000 rpm, while the mass ratio of the disk and the shaft is 0.4.

Keywords: Jeffcott rotor, Lagrangian, fluid film bearings, whirl orbits

Introduction

Rotating shafts are employed in industrial machines such as steam and gas turbines, turbo generators and internal combustion engines. It is important to study the behaviour of these systems under various conditions, especially when there are vibrations on the bearing base. High speed rotors in a jet engine or turbopumps used in space are mostly operated at supercritical speeds, and their bearings and housings are usually supported

resiliently from the frame in order to reduce critical speeds. However, when the aircraft or the space vehicle turns or responds to disturbances, the rotor may be brought into contact with the casing, or the bearings may be damaged due to the vibration caused by gyroscopic movements or centrifugal force.

Fluid film bearings are commonly used in heavy rotating machines because they possess

¹ Department of Mechanical Engineering/Al-Huson University Collage/Al-Balqa' Applied University P.O.Box: 50, Al Huson, Jordan. E-mail: tahat@huson.edu.jo; hwedyan2000@yahoo.com

² School of Engineering, Swinburne University of Technology (Sarawak Camps), Jalan Simpang Tiga, 935576 kuching, Sarawak, Malaysia. E-mail: smutasher@swinburne.edu.my, Tel.: +6082416353/ext507; Fax.: +6082423594.

* Corresponding author

not only high load carrying capacity but also inherent damping properties. Unlike rolling element bearings, fluid film bearings, which are an important machine elements, offer, in addition to support stiffness, substantial damping to insure rotor dynamic stability. The stiffness and damping properties of the fluid film significantly alter the critical speeds and unbalance response of a rotor, lowering its critical speed by up to 25% in practice (Lee, 1993). The studies were carried out on the vibration of a system subjected to translational or rotational motions (Tamura, 1981; Koike and Ishihara, 1983, 1984; Soni and Srinivasan, 1983; Azuma and Saito, 1984; Ehrich, 1989; Al-Bedoor, 2000), in view of the importance for predicting the vibration phenomena of rotor systems subjected to base excitation. Whirling motion is also studied extensively in different drilling processes due to its effect on the outcome surface irregularities. Rotor systems with bearing clearances have been studied in the past, where the investigations concentrated primarily on the Jeffcott rotors. In particular, (Childs, 1982; Choy and Padovan, 1987; Muszynska and Goldman, 1995; Chu and Zhang, 1997, 1998) paid attention to rub interactions in rotating machinery. (Ehrich, 1992) investigated spontaneous side banding, while (Ganesan, 1996) looked at the stability analysis. Synchronous and sub harmonic responses were also investigated (Childs, 1982; Diken, 2001; Ding *et al.*, 2002; Von Groll and Ewins, 2002). Numerical investigation of the Jeffcott rotor model with a snubber ring by Karpenko *et al.* (2002) has

shown the existence of multiple attractors and fractal basins of attraction. Influence of the preloading and viscous damping of the snubber ring was investigated (Karpenko *et al.*, 2003) where it was shown how the preloading could stabilize the dynamic response. Gonsalves *et al.* (1995) designed an experimental rig to simulate the Jeffcott model and made a preliminary comparative analysis between the experimental and numerical results.

In this paper, the dynamic analysis was performed on the vibration of a rigid rotor system with a base of fluid film bearings subjected to vibrations. The resulting model was simulated by using SIMULINK under Matlab software. The responses of the two coordinates (Z and Y) were also observed as well as the whirl orbits of the shaft for different mass ratios.

Model Analysis

The unbalance of high-speed rotors is usually assumed to be very small, and the effect of unbalanced mass on the vibration of a high speed rigid rotor can be neglected (Al-Bedoor, 2000). A schematic representation of the rotor system subjected to a vibrating base of a fluid film bearing is shown in Figures 1(a-b). A rigid rotating shaft with a rigid rotating disk is supported by the fluid film bearing, which is resting on a base that is subject to vibrations. The coordinate system Y and Z is indicated in Figure 1. The kinetic energy of the system is as follows:

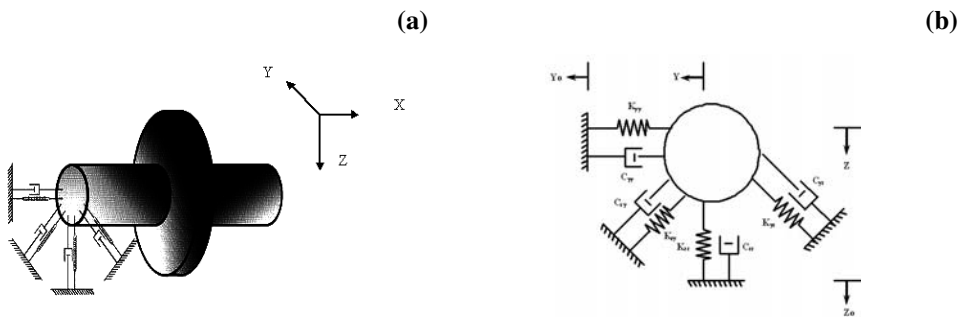


Figure 1. (a) The model of the Jeffcott rotor, (b) A front view of the model for the response analysis, where $y_0 = \sin\omega t$ and $z_0 = \cos\omega t$

$$T = \frac{1}{2} m_s (\dot{y}^2 + \dot{z}^2) + \frac{1}{2} m_d (\dot{y}^2 + \dot{z}^2) \quad (1) \quad \begin{bmatrix} m_s + m_d & 0 \\ 0 & m_s + m_d \end{bmatrix} \begin{bmatrix} \ddot{y} \\ \ddot{z} \end{bmatrix} + \begin{bmatrix} c_{yy} + c_{zy} & c_{yz} \\ c_{zy} & c_{zz} + c_{yz} \end{bmatrix}$$

The potential energy for the system is:

$$U = \frac{1}{2} k_{zz} (z - z_\bullet)^2 + \frac{1}{2} k_{yy} (y - y_\bullet)^2 + \frac{1}{2} k_{zy} (y^2 + z^2) + \frac{1}{2} k_{yz} (y^2 + z^2) \quad (5) \quad \begin{bmatrix} \dot{y} \\ \dot{z} \end{bmatrix} + \begin{bmatrix} k_{yy} + k_{zy} & k_{yz} \\ k_{zy} & k_{zz} + k_{yz} \end{bmatrix} \begin{bmatrix} y \\ z \end{bmatrix} = \begin{bmatrix} c_{yy} \dot{y}_\bullet & k_{yy} y_\bullet \\ c_{zz} \dot{z}_\bullet & k_{zz} z_\bullet \end{bmatrix}$$

$$= \frac{1}{2} k_{zz} (z^2 - 2zz_\bullet + z_\bullet^2) + \frac{1}{2} k_{yy} (y^2 - 2yy_\bullet + y_\bullet^2) + \frac{1}{2} k_{zy} (y^2 + z^2) \quad (2)$$

with the viscous damping coefficients of the bearing denoted c_{zz} , c_{yy} , c_{yz} , c_{zy} , the Raleigh dissipation function of the system can be expressed as:

$$F = \frac{1}{2} c_{zz} (\dot{z} - \dot{z}_\bullet)^2 + \frac{1}{2} c_{yy} (\dot{y} - \dot{y}_\bullet)^2 + \frac{1}{2} c_{zy} (\dot{y}^2 + \dot{z}^2) + \frac{1}{2} c_{yz} (\dot{y}^2 + \dot{z}^2) \quad (3)$$

The Lagrange equation is

$$\frac{d}{dt} \left(\frac{\partial T}{\partial \dot{q}_i} \right) - \left(\frac{\partial T}{\partial q_i} \right) + \frac{\partial F}{\partial \dot{q}_i} + \frac{\partial U}{\partial q_i} = 0.0 \quad (4)$$

where, $q_i = y$ and z

Substituting equations 1, 2, and 3 into equation 4 and after simplification of equation 4, two-coupled equations in y and z direction are formed and the matrix form of these two equations is as follows:

$$M \ddot{X} + C \dot{X} + KX = F(t), \quad (6)$$

where,

$$M = \begin{bmatrix} m_s + m_d & 0 \\ 0 & m_s + m_d \end{bmatrix},$$

$$C = \begin{bmatrix} c_{yy} + c_{zy} & c_{yz} \\ c_{zy} & c_{zz} + c_{yz} \end{bmatrix}$$

$$K = \begin{bmatrix} k_{yy} + k_{zy} & k_{yz} \\ k_{zy} & k_{zz} + k_{yz} \end{bmatrix},$$

$$F(t) = \begin{bmatrix} c_{yy} \dot{y}_\bullet & k_{yy} y_\bullet \\ c_{zz} \dot{z}_\bullet & k_{zz} z_\bullet \end{bmatrix}, X = \begin{bmatrix} y \\ z \end{bmatrix}$$

Using Simulink under Matlab software, to simulate the response of the rotor by, entering the appropriate values for the stiffness and the damping coefficients from Figures 4 and 5. The Simulink model in Figure 2 presents the simulation process for equation 5.

Stability Analysis

When the load and the rotational speed do not fluctuate with time, the journal centre maintains a steady state equilibrium position in the bearing clearance, which is defined uniquely by the Sommerfield number, which represents the operating condition. The equation of motions with respect to the equilibrium state is given as in equation 7:

$$\begin{bmatrix} m_s + m_d & 0 \\ 0 & m_s + m_d \end{bmatrix} \begin{bmatrix} \ddot{y} \\ \ddot{z} \end{bmatrix} + \begin{bmatrix} c_{yy}(\omega) + c_{zy}(\omega) \\ c_{zy}(\omega) \end{bmatrix} \begin{bmatrix} \dot{y} \\ \dot{z} \end{bmatrix} + \begin{bmatrix} c_{zz}(\omega) + c_{yz}(\omega) \\ c_{yz}(\omega) + c_{zz}(\omega) \end{bmatrix} \begin{bmatrix} y \\ z \end{bmatrix} = \begin{bmatrix} F_y \\ F_x \end{bmatrix} \quad (7)$$

Substituting $Y = ye^{\lambda t}$ and $Z = ze^{\lambda t}$ into the homogenous part of equation 7 we get:

$$\begin{bmatrix} M\lambda^2 + (c_{yy} + c_{zy})\lambda + (k_{yy} + k_{zy}) & \\ & k_{zy} + c_{zy}\lambda \\ c_{yz}\lambda + k_{yz} & \\ M\lambda^2 + (c_{zz} + c_{yz})\lambda + (k_{zz} + k_{yz}) & \end{bmatrix} \begin{bmatrix} y \\ z \end{bmatrix} = \begin{bmatrix} 0.0 \\ 0.0 \end{bmatrix} \quad (8)$$

The invariant solution for equation 8 yields:

$$a_0 \lambda^4 + a_1 \lambda^3 + a_2 \lambda^2 + a_3 \lambda + a_4 = 0.0 \quad (9)$$

where,

$$\begin{aligned} a_0 &= M^2 = (m_s + m_d)^2 \\ a_1 &= M(c_{yy} + c_{zy} + c_{zz} + c_{yz}) \\ a_2 &= M(k_{yy} + k_{zy} + k_{zz} + k_{yz}) - c_{zy}c_{yz} + (c_{zz} + c_{yz})(c_{yy} + c_{zy}) \\ &= M(k_{yy} + k_{zy} + k_{zz} + k_{yz}) + c_{zz}c_{yy} + c_{zz}c_{zy} + c_{yz}c_{yy} \\ a_3 &= -(c_{zz} + c_{zy})(k_{yy} + k_{zy}) - (k_{zz} + k_{yz})(c_{yy} + c_{zy}) + k_{zy}c_{yz} \\ a_4 &= -(k_{zz} + k_{yz})(k_{yy} + k_{zy}) + k_{zy}k_{yz} \end{aligned}$$

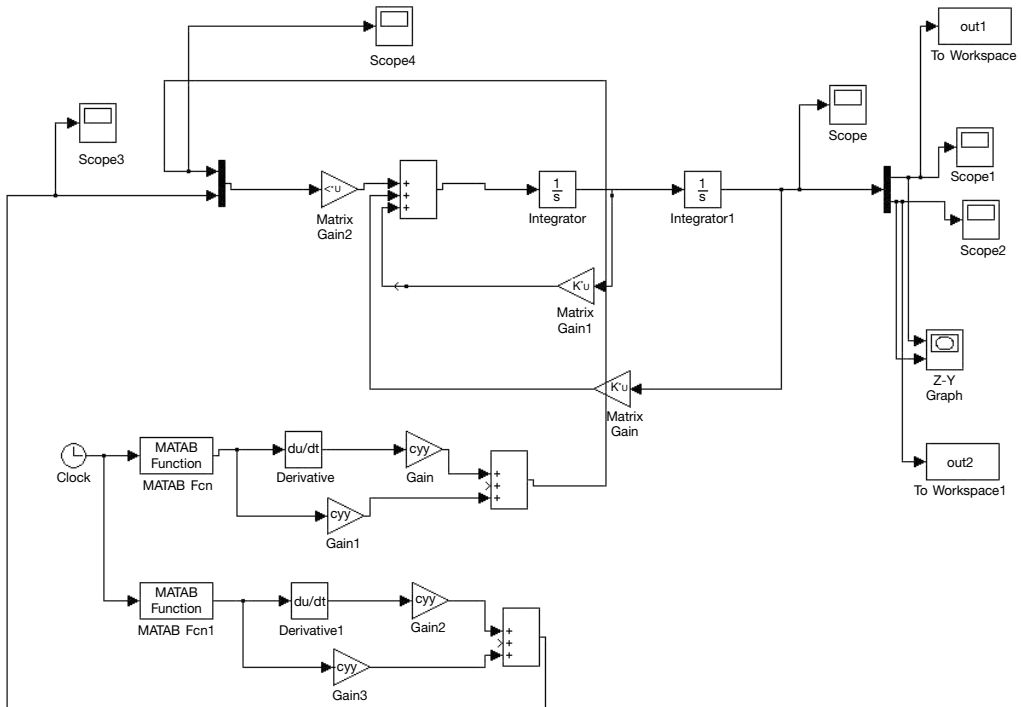


Figure 2. Simulink model for the rotor system

Note that a_i , $i = 1, 2, 3, 4$ are now function of ω . For stability, it is required that:

$$a_1 > 0.0; \quad a_2 > 0.0; \quad a_3 > 0.0;$$

$$a_4 > 0.0; \quad a_1 a_2 - a_0 a_3 > 0.0; \quad \text{and}$$

$$a_1 a_2 a_3 - a_3^2 a_0 - a_1^2 a_4 > 0.0 \tag{10}$$

At the onset of instability ($\lambda = iv$), means the whirl at the boundary of the stable region. By substituting $\lambda = iv$ in equation 9 and equating real and imaginary parts to zero:

$$a_0 v^4 - a_2 v^2 + a_4 = 0.0 \tag{11}$$

$$iv (-a_1 v^2 + a_3) = 0.0 \tag{12}$$

Therefore, at the stability limit, the frequency of whirl approaches

$$v^2 = \left[\frac{a_3}{a_1} \right]_{\omega=\omega_{th}} \tag{13}$$

If the threshold speed ω_{th} exists, the unstable vibration is satisfies

$$a_1 a_2 a_3 - a_3^2 a_0 - a_1^2 a_4 = 0.0 \tag{14}$$

Note that the stability limit condition in equation 14 is obtained by substituting equation 13 into equation 11. In other words, at the rotational speed $\omega = \omega_{th}$, the stability limit is encountered and the unstable whirl frequency is given by equation 13. In particular, the threshold speed and whirl frequency can also be obtained by using dimensionless bearing stiffness and damping coefficients and equations 13 and 14 as follows:

$$a_0 = \left[\frac{W}{g} \right]^2, \quad a_1 = \left[\frac{W^2}{gC\omega} \right] A_1,$$

$$a_2 = \left[\frac{W^2}{gC} \right] A_2 + \left[\frac{W}{C\omega} \right]^2 A_3$$

$$a_3 = \left[\frac{W^2}{C^2\omega} \right] (A_4 + A_5 + A_6)$$

$$a_4 = \left[\frac{W}{C} \right]^2 A_7 \tag{15}$$

Substituting equation 15 into equations 13 and 14 one can find the threshold speed

$$\omega_{th}^{*2} = \omega_{th} \left[\frac{C}{g} \right] = \tag{16}$$

$$\frac{A_1 A_2 (A_4 + A_5 + A_6)}{(A_4 + A_5 + A_6)^2 + A_1^2 A_7 - A_1 A_2 (A_4 + A_5 + A_6)}$$

and then the unstable whirl frequency

$$v_{th}^{*2} = \left[\frac{A_4}{A_1} \right]_{\omega^*=\omega_{th}^*} \tag{17}$$

Here:

$$\omega^* = \omega \sqrt{\frac{C}{g}}, \quad v_{th}^* = v_{th} \sqrt{\frac{C}{g}}$$

$$A_0 = \left[\frac{W}{g} \right]^2$$

$$A_1 = (c_{yy} + c_{zy} + c_{zz} + c_{yz})$$

$$A_2 = (k_{yy} + k_{zy} + k_{zz} + k_{yz})$$

$$A_3 = (c_{zz} c_{yy} + c_{zz} c_{zy} + c_{yz} c_{yy})$$

$$A_4 = -(c_{zz} + c_{zy})(k_{yy} + k_{zy})$$

$$A_5 = -(k_{zz} + k_{yz})(c_{yy} + c_{zy})$$

$$A_6 = k_{zy} c_{yz}$$

$$A_7 = (k_{zz} + k_{yz})(k_{yy} + k_{zy}) - k_{zy} k_{yz}$$

The dimensionless bearing coefficients are

$$K_{ij} = \frac{k_{ij}C}{W}, \quad C_{ij} = \frac{c_{ij}C\omega}{W}, \quad (18)$$

where $i, j = y, z$ and $W = mg$

Equation 18 explains the situation in which a small perturbation increases the vibration amplitudes beyond the threshold speed ω_{th} , which is determined by K_{ij} and C_{ij} . The unstable whirl frequency ν for lightly loaded journal bearings can be obtained as follows: when W (or $1/S$) approaches zero equation 8 may be approximated by:

$$\begin{bmatrix} (c_{yy} + c_{zy})\lambda + (k_{yy} + k_{zy}) \\ k_{zy} + c_{zy} \lambda \\ c_{yz} \lambda + k_{yz} \\ (c_{zz} + c_{yz})\lambda + (k_{zz} + k_{yz}) \end{bmatrix} \begin{bmatrix} y \\ z \end{bmatrix} = \begin{bmatrix} 0.0 \\ 0.0 \end{bmatrix} \quad (19)$$

where

$$S = \frac{\mu NDL}{W} \left[\frac{R}{C} \right]^2$$

Leading to the characteristic equation:

$$a_2' \lambda^2 + a_3 \lambda + a_4 = 0 \quad (20)$$

where

$$a_2' = (c_{yy} + c_{zy})(c_{zz} + c_{yz}) - c_{yz}c_{zy} =$$

$$\left[\frac{W}{C\omega} \right]^2 A_3 + \left[\frac{W^2}{gC} \right] A_2$$

$$a_3 = (c_{yy} + c_{zy})(k_{zz} + k_{yz}) + (k_{yy} + k_{zy})(c_{zz} + c_{yz}) - k_{zy}c_{yz} - k_{yz}c_{zy}$$

$$a_4 = (k_{yy} + k_{zy})(k_{zz} + k_{yz}) - k_{zy}k_{yz}$$

The terms in equation 20 related to the bearing coefficients are to be evaluated at $S = \infty$. For stability, it is then required that $a_2' > 0.0$, $a_3 > 0.0$, $a_4 > 0.0$ since $a_3 = 0.0$ ($A_4 = 0$,

$A_5 = 0$, $A_6 = 0$) at the stability limit, the unstable whirl frequency can be obtained, by substituting $\lambda = i\nu$ into equation 20, i.e.:

$$\nu^2 = \frac{a_4}{a_2'} = \frac{\begin{vmatrix} k_{yy} + k_{zy} & k_{yz} \\ k_{zy} & k_{zz} + k_{yz} \end{vmatrix}}{\begin{vmatrix} c_{yy} + c_{zy} & c_{yz} \\ c_{zy} & c_{zz} + c_{yz} \end{vmatrix}} = \frac{\det(K)}{\det(C)} = (n_\nu \omega)^2 \quad (21)$$

where

$$n_\nu = \frac{1}{\omega} \sqrt{\frac{\det(K)}{\det(C)}}$$

or,

$$\nu^2 = \left[\frac{A_5}{A_3} \right] \omega^2 = \frac{\begin{vmatrix} k_{yy} + k_{zy} & k_{yz} \\ k_{zy} & k_{zz} + k_{yz} \end{vmatrix}}{\begin{vmatrix} c_{yy} + c_{zy} & c_{yz} \\ c_{zy} & c_{zz} + c_{yz} \end{vmatrix}} \omega^2 \quad (22)$$

Therefore the instability for the lightly loaded journal bearings occur when $\det(K)$ and $\det(C)$ evaluated at $S = \infty$ are of the same sign. The synchronous whirl takes place when $n_\nu = 1$. When $n_\nu > 1$ ($n_\nu < 1$), super synchronous (sub synchronous) whirl occurs and the corresponding critical case will be encountered at the rotational speed equal to $\frac{1}{n_\nu}$ times the flexural critical for a flexible rotor.

Results and Discussions

The response and the whirl orbit of the system at $\omega = 8,000$ rpm, the mass of the shaft and the disk were changed and the values of the stiffness and the damping coefficients were taken from Figures 4 and 5 respectively, as shown in Figure 3. When the system was considered as a light rotor, the whirl orbit was inclined with an angle equal to 143° and the aspect ratio (r_{min}/r_{max}) is 0.25. The result of the inclination angle is

acceptable compared to the value obtained in (Ehrich, 1989) which is 135° for the same values of the coefficients and this is due to the vibration of the base in the z and y directions, taken as harmonic excitation with the same amplitude. Also, as can be seen from Figure 3, there is no transient, so the system goes to a stable position. In order to study the effect of disk mass on the stability of the system, the shaft mass is kept constant and the mass of the disk for the same rotational speed is change. Figure 6 shows the response and the whirl orbit of the system. It is observed that the transient motion of the system was increased but the system will finally go to the steady state motion. By continuously increasing the disk mass the transient motion was longer as shown in Figure 7. Figure 8 shows the response of the maximum mass of the disk. It is clear that increasing the disk mass will increase the time of transient motion. The effect of the damping on the response of the system is presented in Figure 9, if the damping coefficients are $C_{yy} = C_{zz} = C_{zy} = C_{yz} = 0.0$, the system will not be stable as shown in Figure 9. Figure 10 shows the response of the system assuming that all the stiffness and damping coefficients are the same $C_{yy} = C_{zz} = C_{zy} = C_{yz}$ and $K_{yy} = K_{zz} = K_{zy} = K_{yz}$, the amplitude of the motion in y and z direction is 1.50 mm and 0.41 mm respectively, the inclination angle of the whirl orbit is 143° and the aspect ratio is 0.27. Figure 11 shows the response of the system assuming $C_{zy} = C_{yz}$ and $K_{zy} = K_{yz}$, the amplitude of the motion in y and z direction is 0.65 mm and 2.00 mm, respectively; the inclination angle of the orbit is 137° and the aspect ratio is 0.32. When there is no cross coupling in the system, i.e. $C_{zy} = C_{yz} = K_{zy} = K_{yz} = 0$ and $K_{zz} = K_{yy}$, $C_{zz} = C_{yy}$ the whirl shape will be circular as shown in Figure 12. The inclination angle here is equal to zero and the amplitude in y and z directions is 2.00 mm and 0.5 mm, respectively.

Conclusions

The whirl motion of the Jeffcott rotor was investigated. The simulation was carried out under a constant rotational speed and different

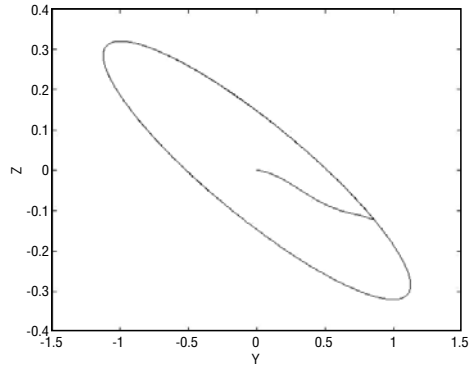


Figure 3. Whirl orbit at $\omega = 8,000$ rpm, mass of disk = 40 kg, mass of shaft = 100 kg

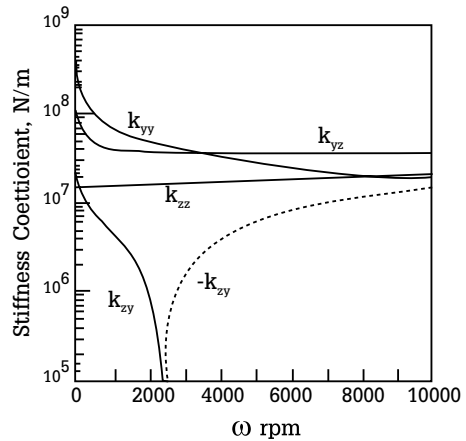


Figure 4. Stiffness coefficient as a function of ω , $L/D = 0.25$, [1]

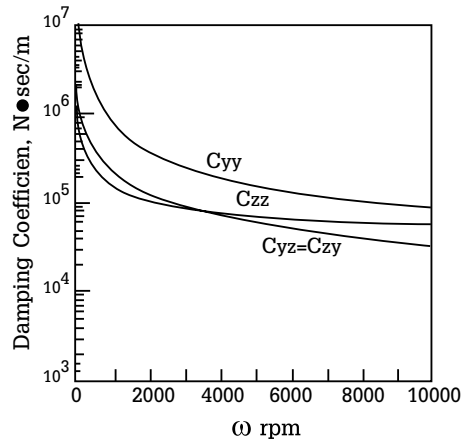


Figure 5. Damping coefficients as a function of ω , $L/D = 0.25$, [1]

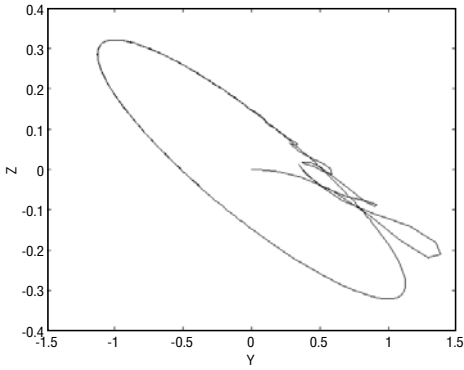


Figure 6. Whirl orbit at $\omega = 8,000$ rpm, mass of disk = 10,000 kg, mass of shaft = 100 kg

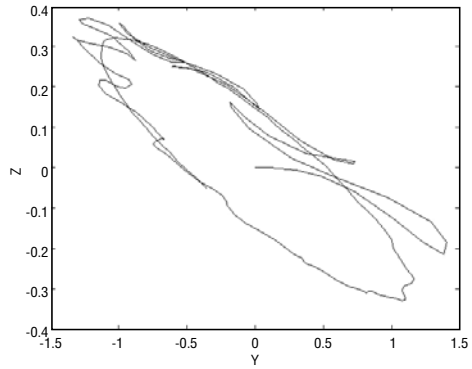


Figure 7. Whirl orbit at $\omega = 8,000$ rpm, mass of disk = 80,000 kg, mass of shaft = 100 kg

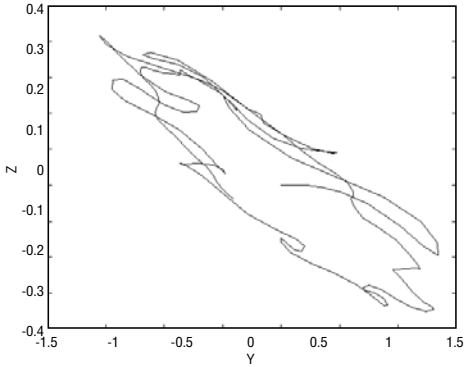


Figure 8. Whirl orbit at $\omega = 8,000$ rpm, mass of disk = 150,000 kg, mass of shaft = 100 kg

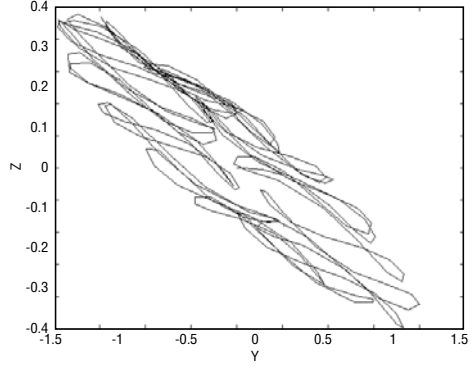


Figure 9. Whirl orbit at $\omega = 8,000$ rpm, mass of disk = 20,000 kg, mass of shaft = 50,000 kg without damping ($c_{yy} = c_{zz} = c_{zy} = c_{yz} = 0.0$)

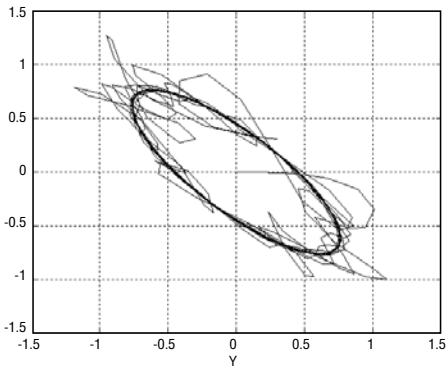


Figure 10. Whirl orbit at $\omega = 8,000$ rpm, mass of disk = 200,000 kg, mass of shaft = 100,000 kg ($c_{yy} = c_{zz} = c_{zy} = c_{yz}$, $k_{zz} = k_{yy} = k_{zy} = k_{yz}$)

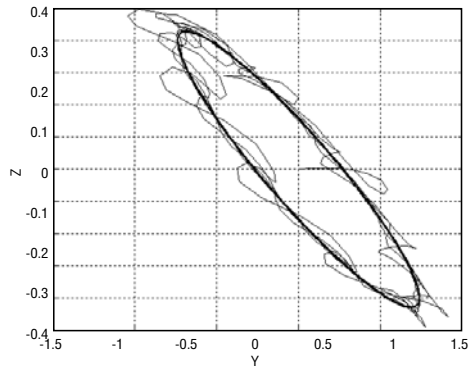


Figure 11. Whirl orbit at $\omega = 8,000$ rpm, mass of disk = 200,000 kg, mass of shaft = 100,000 kg ($c_{zy} = c_{yz}$, $k_{zy} = k_{yz}$)

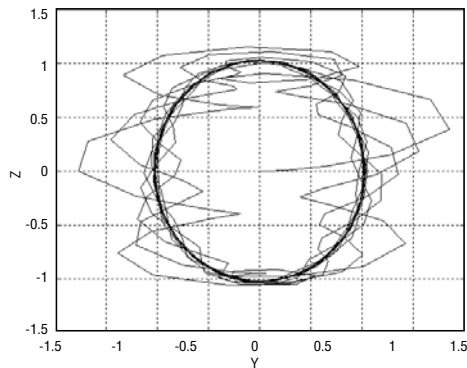


Figure 12. Whirl orbit at $\omega = 8,000$ rpm, mass of disk = 200,000 kg, mass of shaft = 100,000 kg ($c_{zy} = c_{yz} = k_{zy} = k_{yz} = 0$, $k_{zz} = k_{yy}$, $c_{zz} = c_{yy}$)

masses for the shaft and the disk. The responses of the two coordinates (Z and Y) were also observed as well as the whirl orbits of the shaft for different mass ratios. Furthermore, the stability of the system was investigated. The conclusions are summarized as follows:

1. The results show that the whirl motion is stable when the rotor speed is 8,000 rpm, while the mass ratio of the disk and shaft are 0.4.
2. The whirl shape was circular when there is no cross coupling in the system.
3. The rotors are not stable where there is no damping in the system.
4. A comparison of current results with the results in the literature is acceptable.

Nomenclatures

C : Clearness
 C_{ij} : Damping coefficients
 D : Diameter of the bearing
 Det : Determent
 g : Gravitational acceleration
 K_{ij} : Stiffness coefficients
 L : length of the shaft
 m_s : The mass of the shaft
 m_d : The mass of the disk
 R : Radius of the bearing
 S : Sommerfield number
 W : The bearing radial load
 Y : The base excitation in Y- direction

Z : The base excitation in Z- direction
 ν : Frequency of whirl
 ν_{th}^* : Unstable whirl frequency

Greek Letters

ω_{th} : threshold speed
 ω : Rotational speed of the shaft
 μ : Viscosity of the lubricant

References

- Al-Bedoor, B.O. (2000). Transient torsional and lateral vibrations of unbalanced rotors with rotor-to-stator rubbing. *J. Sound and Vibrat.*, 229(3):627-645.
- Azuma, T. and Saito, S. (1984). Seismic response analysis of a rotor system by complex modal method. *Transactions of Japan Society of Mechanical Engineers, Series C*, 50(460):2,242-2,248.
- Chu, F. and Zhang, Z. (1997). Periodic quasi-periodic and chaotic vibrations of a rub-impact rotor system supported on oil film bearing. *Int. J. Eng. Sci.*, 35(10-11):963-973.
- Chu, F. and Zhang, Z. (1998). Bifurcation and chaos in a rub-impact Jeffcott rotor system. *J. Sound Vibrat.*, 210(1):1-18.
- Childs, D.W. (1982). Fractional-frequency rotor motion due to non-symmetric clearance effects. *J Eng Power Trans. ASME*, 104: 533-541.
- Choy, K. and Padovan, J. (1987). Non-linear transient analysis of rotor-casing rub events. *J. Sound Vibrat.*, 113(3):529- 545.
- Diken, H. (2001). Non-linear vibration analysis and sub harmonic whirl frequencies of the Jeffcott rotor model. *J. Sound Vibrat.*, 243(1):117-125.
- Ding, Q., Cooper, J. E., and Leung, A. Y. T. (2002). Hopf bifurcation analysis of a rotor/seal system, *J. Sound Vibrat.*, 252(5):817-833.
- Ehrich, F. F. (1989). The role of bearing support stiffeners anisotropy in suppression of rotor dynamic instability. *Proceedings of the 1989 Design Technical Conferences-12th Biennial Conference on Mechanical Vibration and Noise, Montreal; Sept 17-21,*

- 1989; Quebec, Canada, p. 160-166.
- Ehrich, F. (1992). Spontaneous sidebanding in high-speed rotordynamics. *J. Vib. Acoust.*, 114:498-505.
- Ganesan, R. (1996). Dynamic response and stability of a rotor-support system with non-symmetric bearing clearances, *Mechanism Machine Theory*, 31(6): 781-798.
- Gonsalves, D., Neilson, R., and Barr, A. (1995). A study of response of a discontinuously nonlinear rotor system. *Nonlinear Dynamics*, 7:451-470.
- Karpenko, E., Pavlovskaja, E., and Wiercigroch, M. (2003). Bifurcation analysis of a preloaded Jeffcott rotor. *Chaos, Solitons & Fractals*, 15(2):407-416.
- Karpenko, E., Wiercigroch, M., and Cartmell, M. (2002). Regular and chaotic dynamics of a discontinuously nonlinear rotor system, *Chaos, Solitons & Fractals*, 13(6):1,231-1,242.
- Koike, H. and Ishihara, K. (1983). Impact response of a rotor-bearing system subjected to a base excitation (first report). *Transactions of Japan Society of Mechanical Engineers, Series C*, 49(438):173-181.
- Koike, H. and Ishihara, K. (1984). Impact response of a rotor-bearing system subjected to a base excitation (second report). *Transactions of Japan Society of Mechanical Engineers, Series C*, 50(478): 470-478.
- Lee, C.W. (1993). *Vibration Analysis of Rotors*. (3rd ed.), Kluwer Academic Publisher, Boston, USA, 332 p.
- Muszynska, A. and Goldman, P. (1995). Chaotic responses of unbalanced rotor/bearing/stator systems with looseness or rubs. *Chaos, Solitons & Fractals*, 5(9):1,683-1,704.
- Sakata M., Kimura, K., Okamoto, S., and Oikawa, K. (1995). Vibration Analysis of a high speed and light weight rotor system subjected to a pitching or turning motion, I: A rigid rotor system on flexible suspensions. *J. Sound Vibrat.*, 184(5):871-885.
- Soni, A.H. and Srinivasan, V. (1983). Seismic analysis of a gyroscopic mechanical system. *Transactions of American Society of Mechanical Engineers, J. Vib. Acoust. Stress Reliab. Des.*, 105:449-455.
- Tamura, A. and Kanai, S. (1981). Steady response of rotor on flexible suspensions subjected to base excitation. *Transactions of the Japan Society of Mechanical Engineers, Series C*, 47(424):1,586-1,592.
- Von Groll, G. and Ewins, D.J. (2002). A mechanism of low subharmonic response in rotor/stator contact - measurements and simulations. *J. Vib. Acoust.*, 124:350-358.